

Capturing Near-Earth Asteroids Using A Binary Exchange Mechanism

Andy Borum, James Burns, Peter Wentzel, Aleksandr Andreyev

Advisor- Dr. Shane Ross

Department of Engineering Science and Mechanics

Virginia Polytechnic Institute and State University, Blacksburg VA 20406

Abstract

A new method of capturing an asteroid in an orbit around the Earth is proposed, inspired by the theory that the irregular satellites of Jupiter and Neptune may have at one time been members of a binary asteroid. After a close approach with the planet, the binary asteroid was disrupted, and one member was captured into a permanent orbit. A parametric study was conducted by simulating binary-Earth encounters. The total mass of the binary system and the velocity of the binary asteroid relative to the Earth as it enters the Earth's Hill sphere were found to be the two dominant parameters affecting capture. These results were used to select a candidate near-Earth binary asteroid, 1999 HF1, with which additional simulations were conducted. It was found that the candidate asteroid could only be captured with a high probability at low velocities, and the resulting orbits were larger than the Earth's Hill sphere. However, larger non-near-Earth binary asteroids could be captured within the Hill sphere. The effect of treating the larger member of the binary system as an extended body and the effect of the moon were also considered. A close approach with the moon sometimes resulted in one or both binary members being captured within the Hill sphere. A single asteroid can also be captured when it has a close encounter with the moon, suggesting that lunar-encounter driven capture deserves further attention.

Keywords: Binary Asteroids, Asteroid Capture, Binary Exchange, Near-Earth Asteroids

1. Introduction

It has been proposed that many of the irregular satellites within the solar system were not formed by accretion within circumplanetary disks as is the case for regular satellites¹. Instead, irregular satellites are believed to have once been asteroids that were captured into permanent orbits around their respective planets². Various methods describing how these asteroids were captured have been formulated. While these capture mechanisms give us a description of irregular satellite formation in the early solar system, they also provide potential methods by which an asteroid could be captured in an orbit around the Earth. A captured asteroid would have many uses and could offer financial, technological, and political benefits for government agencies or private companies willing to explore this novel resource. The recent decommission

of the NASA space shuttle and the accompanying push by the United States government for private space exploration makes these incentives for private companies particularly interesting.

Having an asteroid in such close proximity to the Earth would provide a rich source of precious metals. Mining the Earth's surface for minerals is destroying ecosystems and causing danger to those who work in or live near these mining sights. Mudslides and contaminated drinking water are just two of the threats posed to residents of mining towns. Environmental devastation is not the only negative effect of excessive mining. If mineral excavation rises just two percent annually, the Earth's supply of accessible lead will be gone in 17 years, tin in 19 years, copper in 25 years, and iron in 54 years³. We must either learn to live within the Earth's limits or find a new source of these raw materials⁴.

A captured asteroid would provide a rich source of these metals^{5,6}. Data captured by the Near Earth Asteroid Rendezvous spacecraft has shown that Eros, a near Earth asteroid, contains more aluminum, gold, silver, and zinc than could ever be mined from the Earth. The economics of mining asteroids has been analyzed and deemed feasible^{7,8,9}. Potential candidates for excavation methods include drilling and magnetic extraction. Both nuclear and solar energy could be used to power these processes. Having access to such a large mineral resource would greatly decrease the strain placed on the Earth to provide raw materials. Ecosystems could be saved from destruction and potential health risks to humans would diminish. By developing the technology to capture an asteroid in an orbit around the Earth, the environmental damage caused by mining could be stopped and a seemingly endless supply of precious metals could be obtained

In addition to improving life on Earth, the captured asteroid would be of great aid in space exploration. Building fueling stations on asteroids would allow for longer and less expensive space exploration missions. A spacecraft could be loaded with only enough fuel to reach the asteroid, thus lightening the load the craft would have to carry out of Earth's atmosphere. After fueling up on the asteroid, the craft could continue on its mission with a full tank. Space stations could also be built on asteroids and act as manufacturing plants for space materials or launch sites for spacecrafts. Building materials on the asteroid using the asteroids rich supply of raw ore would take away the expense of launching the materials out of the atmosphere. Spacecraft being launched from the surface of the asteroid could take advantage of the angular velocity of the asteroid due to its orbit around the Earth.

A captured asteroid would also allow scientists to study the composition of a celestial body without it being distorted by a harsh entry into our atmosphere. Some asteroids are believed to be minimally altered from their state when the solar system first formed. Being able to study such an asteroid would give great insight into the nature and composition of deep space bodies. Lastly, if the situation were to arise, a captured asteroid could be used as a shield to protect the Earth from potentially hazardous objects¹⁰.

Three main problems must be solved in order to bring an asteroid to Earth. The first obstacle involves developing the appropriate control algorithm and acceleration profile needed to steer an asteroid from its current location to the edge of Earth's gravitational influence. Research on this problem was conducted last year by a Virginia Tech senior design team led by Zaki

Hasnain and Chris Lamb¹¹. Their research focused on developing an algorithm that could be used to steer a single asteroid to have a close approach with the Earth. The second challenge is to design and build the machine that will thrust the asteroid towards Earth. Ideas such as a robot that ejects matter gathered from the surface of the asteroid¹⁰ and solar powered drivers¹² have been proposed.

The third problem, which is the focus of this paper, is how to slow down the asteroid to an appropriate speed for it to remain in a stable Earth orbit. Within this report, we propose a new method for capturing a near Earth asteroid by using a binary exchange mechanism. This technique relies on a two asteroid system, known as a binary asteroid, making a close approach to the Earth. This method has been used to explain the formation of the irregular moons of Jupiter^{13, 14} and Neptune^{15,16}. In Section 2, we will first explore binary exchange and other models of asteroid capture that have been proposed. Section 3 provides an overview of the solar system's binary asteroid population and which of these asteroid could be potential candidates for capture. Section 4 formulates the problem and describes the numerical techniques used to conduct the simulations. Section 5 presents results of numerical simulations of binary-Earth encounters for a wide range of binary asteroid parameters and initial conditions. In Section 6, a candidate binary asteroid is chosen based on the results presented in the previous section. Section 7 presents additional simulations of encounters between the candidate asteroid and Earth. In Sections 8 and 9, the effects of treating the larger asteroid as a non-spherical extended body and the effects of the moon are examined, respectively. Concluding remarks are given in Section 10, and acknowledgements are given in Section 11.

2. Previously Proposed Methods of Asteroid Capture

While regular satellites are characterized by nearly circular and uninclined orbits, irregular satellites move along highly eccentric and/or inclined orbits. These differences suggest that the formation mechanisms for each type are different and that irregular satellites were once on hyperbolic orbits and later captured. Four models of capture have been proposed in previous literature:

- (1) Collisions between an asteroid and a planet resulting in a captured satellite
- (2) Capture through dissipation of orbital energy due to gas drag
- (3) Pull-down capture, in which a planet's mass suddenly increases
- (4) Capture through multi-body gravitational interactions

A review of last three methods is given in Jewitt and Haghighipour (2007)¹⁷. In method 1, the size of the asteroid required for capture would be large enough to produce a catastrophic collision, and the ejection speed of large fragments after collision would not be great enough to produce stabilized orbits¹⁸. Studies of gas drag capture have shown that permanent capture due to

gas drag is possible, but unlikely to have occurred in the early solar system¹⁹. Pull-down capture was also shown to be able to produce capture in a Sun-Jupiter-Satellite environment²⁰.

Clearly, methods 1 and 3 are not reasonable methods for capturing an asteroid around the Earth. Also, method 2 would be very difficult to implement, as a spherical dust cloud would need to be created around the Earth. Thus, method 4 is the most feasible method for Earth capture. One type of gravitational capture occurs when a satellite interacts with two planets and becomes bound to one of the planets. It has been shown that in the early solar system, encounters between the outer planets within the planetesimal disk could have resulted in capture¹⁸. It has also been shown that planetary resonance could lead to irregular satellite capture²¹.

The most feasible mechanism to implement in an Earth environment is binary exchange. This method has been used to explain the capture of Triton by Neptune^{15,16} and the irregular moons of Jupiter^{13,14}. This method relies on a close encounter between a two member system, known as a binary asteroid, and a planet. If the binary asteroid is oriented correctly when it makes its closest approach to the planet, one of the two asteroids could be moving slowly enough relative to the planet to be captured. This method of capture was examined in an Earth environment for a wide range of binary asteroid parameters and initial conditions. A schematic illustration of binary exchange is shown in Figure 1.

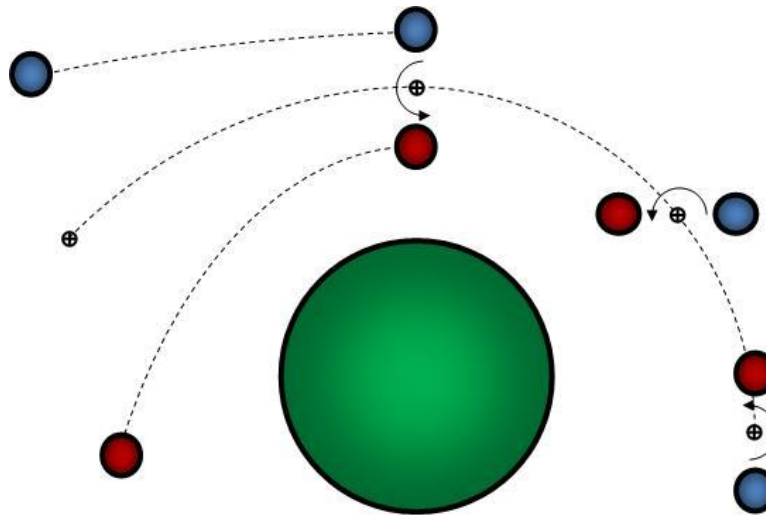


Figure 1. Schematic of Binary Exchange (Movie available at <http://www.youtube.com/watch?v=n6A8xAcf2VA>)

3. Binary Asteroid Population

A binary asteroid is comprised of two asteroids that orbit their center of mass as the system follows some larger orbit. In Pravec and Harris (2007)²², an overview of the characteristics of 73 binary asteroids is given, including the 36 known near-Earth binary asteroids. For the entire population surveyed, the total mass of binary systems ranges from 3.1×10^9 kg to 2.6×10^{19} kg, the mass ratio, defined as ratio of the mass of the larger member to the mass of both members,

ranges from 0.5 to 0.999, and the binary semi-major axes range from 500 m to 3400 km. The orbital eccentricity of the mutual binary orbit of the majority of binary asteroids is very small.

Simulations were conducted using these parameter ranges; however, the 36 near-Earth asteroids were only considered as potential candidates for capture. The process of steering a binary asteroid from its current orbit to an orbit with a close encounter with the Earth was left for future work. Given their proximity, near-Earth binary asteroids would be the easiest to steer to the Earth. The near-Earth binary asteroids have total masses ranging from 3.1×10^9 kg to 6.7×10^{13} kg, mass ratios ranging from 0.578 to 0.999, and semi-major axes ranging from 500 m to 6 km. The total masses, mass ratios, and semi-major axes of the near-Earth binary asteroids are presented in Appendix 1.

4. Problem Formulation

Simulations were conducted using a six stage adaptive step size Gragg-Bulirsch-Stoer integration scheme constructed using Matlab²³. An overview of this numerical integration technique is given in Appendix 2. To check the accuracy of the simulations, the relative change in total energy was tracked, and was found to never vary by more than 10^{-6} . The simulations were run for 6×10^6 seconds. Binary parameters and initial conditions were selected using a Latin hypercube sampling technique in order to efficiently span the parameter space²⁴. The equations of motion governing the binary-Earth system are,

$$\begin{aligned} \dot{\bar{\mathbf{x}}}_e &= \bar{\mathbf{v}}_e & \ddot{\bar{\mathbf{x}}}_e &= G \left(\frac{M_1(\bar{\mathbf{x}}_1 - \bar{\mathbf{x}}_e)}{|\bar{\mathbf{r}}_{e1}|^3} + \frac{M_2(\bar{\mathbf{x}}_2 - \bar{\mathbf{x}}_e)}{|\bar{\mathbf{r}}_{e2}|^3} \right) \\ \dot{\bar{\mathbf{x}}}_1 &= \bar{\mathbf{v}}_1 & \ddot{\bar{\mathbf{x}}}_1 &= G \left(\frac{M_e(\bar{\mathbf{x}}_e - \bar{\mathbf{x}}_1)}{|\bar{\mathbf{r}}_{e1}|^3} + \frac{M_2(\bar{\mathbf{x}}_2 - \bar{\mathbf{x}}_1)}{|\bar{\mathbf{r}}_{12}|^3} \right) \\ \dot{\bar{\mathbf{x}}}_2 &= \bar{\mathbf{v}}_2 & \ddot{\bar{\mathbf{x}}}_2 &= G \left(\frac{M_e(\bar{\mathbf{x}}_e - \bar{\mathbf{x}}_2)}{|\bar{\mathbf{r}}_{e2}|^3} + \frac{M_1(\bar{\mathbf{x}}_1 - \bar{\mathbf{x}}_2)}{|\bar{\mathbf{r}}_{12}|^3} \right) \end{aligned} \quad (1)$$

with respect to an Earth centered frame. The subscript e denotes the Earth, and the subscripts 1 and 2 denote the larger and smaller members of the binary asteroid, respectively.

The variables within each simulation were the total mass of the two asteroid system, M_{tot} , the mass ratio, \mathcal{C} , as defined earlier, the velocity of the binary system at an infinite distance away from the earth, v_∞ , from which the initial velocity v_0 is derived, the closest approach of the binary center of mass to the Earth, r_p , from which an angle ϕ orienting v_0 is derived, the initial semi-major axis of the mutual binary orbit, a , the initial eccentricity of the mutual binary orbit, e , one angle prescribing the true anomaly, θ , three angle prescribing the orientation of the binary orbit, α, β, γ , and a variable determining the direction in which the binary rotates, g . A schematic showing these initial conditions and binary parameters relative to the binary center of mass is shown in Figure 2.

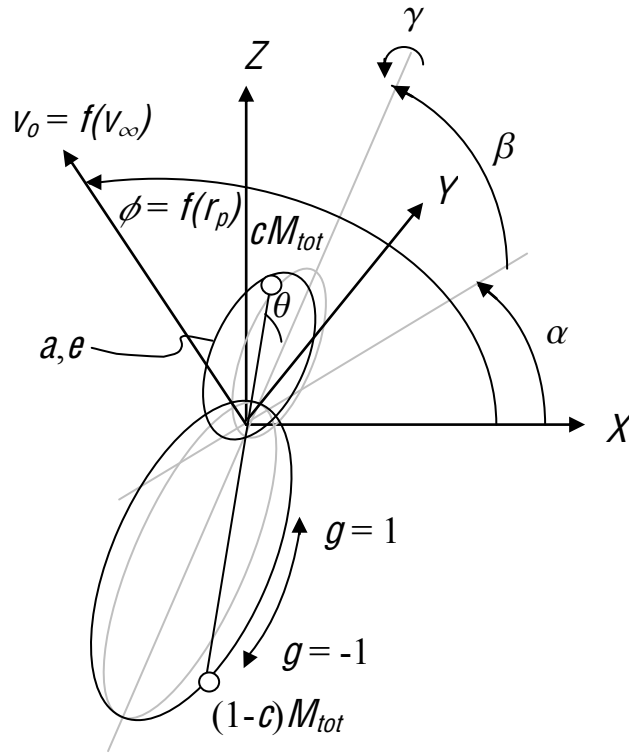


Figure 2. Schematic of Initial Conditions Relative to Binary Center of Mass

The asteroids were assumed to have a density of 3 g/cm^3 and were initially located at the edge of the Earth's Hill sphere. The variables were varied across the following ranges: $M_{tot} \in [10^8 \text{ kg}, 10^{20} \text{ kg}]$, $c \in [0.5, 0.99]$, $v_\infty \in [0 \text{ m/s}, 100 \text{ m/s}]$, $r_p \in [2R_e, 60R_e]$, $a \in [4R_1, 16R_1]$, $e \in [0, 0.8]$, $\theta, \alpha, \beta, \gamma \in [0, 2\pi]$, and $g = -1$ or 1 , where R_e is the radius of the Earth and R_1 is the radius of the larger asteroid. After each time step, the distance between the two asteroids was compared with the sum of the asteroid's radii. If the distance was less than this sum, the simulation was marked as resulting in a collision. Figure 3 shows one simulation in which capture occurred and the resulting orbit was contained within the Earth's Hill sphere. For this simulation, $M_{tot} = 5.94 \times 10^{17} \text{ kg}$, $c = 0.95$, $v_\infty = 100 \text{ m/s}$, $r_p = 2R_e$, $a = 1.5R_1$, $e = 0$, $\theta = 1.8$, $\alpha = 0$, $\beta = 0$, $\gamma = 0$, and $g = 1$.

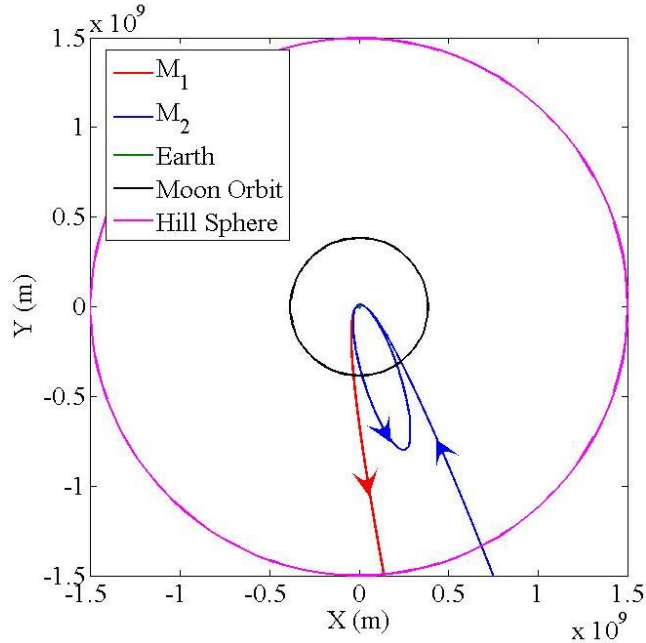


Figure 3. Example of Asteroid Capture Through Binary Exchange (Movie available at <http://www.youtube.com/watch?v=hg1IfW Ks3bc>)

In Figure 3, the Earth's Hill sphere is shown by the purple circle. In order for an asteroid to remain on a stable orbit around the Earth, the asteroid's orbit must not extend beyond the Earth's Hill sphere, which has a radius of 1.5×10^9 m, or roughly 235 Earth radii. Once the asteroid leaves the Earth's Hill sphere, the effect of other bodies such as the sun can perturb the asteroids and render it unbound from the Earth.

5. Results of Parametric Study

The following plots represent results from 100,000 simulations. First, the effect of each variable on the probability of capture was examined. An asteroid was considered captured if the semi-major axis of its final orbit around the Earth was positive. Whether the orbit was contained within the Earth's Hill sphere was not considered when computing the probability of capture. Figure 4 shows plots of the probability of capture as a function of the variables $\log(M_{tot})$, \mathcal{C} , v_{∞} , r_p , a , and θ for the larger of the two asteroids, while Figure 5 shows the same plots for the smaller of the two.

The probability of capturing the smaller of the two asteroids is higher than that of capturing the larger asteroid in all cases. It can be seen that v_{∞} and M_{tot} have the most profound effect on the probability of capture, with the probability decreasing as v_{∞} is increased and increasing as M_{tot} is increased. The probability is also seen to decrease with increasing r_p and θ for both asteroids. Increasing a and \mathcal{C} causes an increase in the probability of capture.

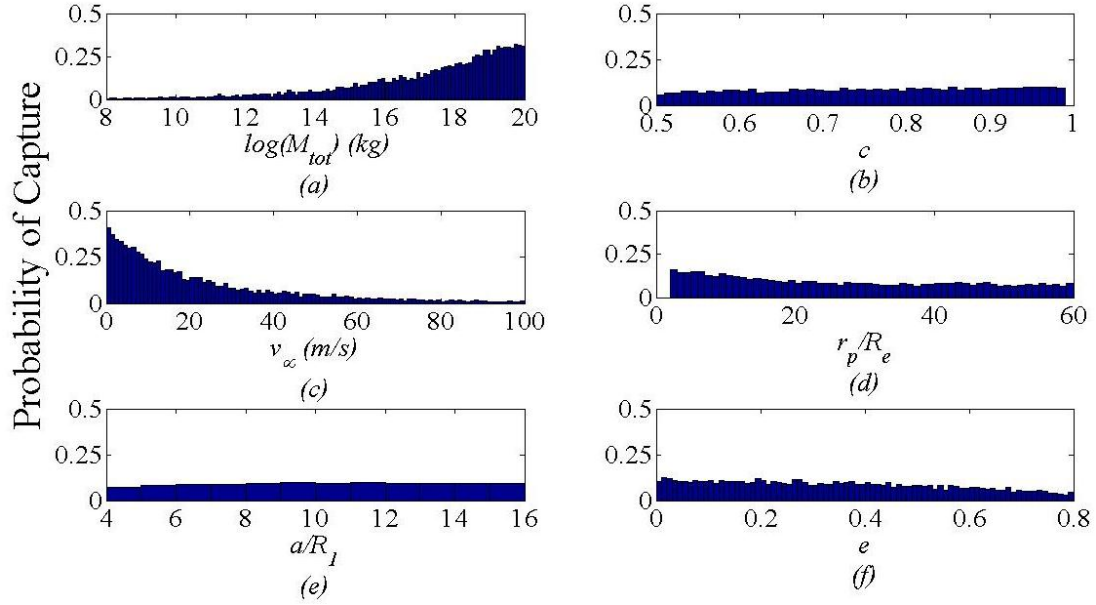


Figure 4. Probability of Capture as a Function of the System Variables for Larger Binary Member. (a) Total Mass, (b) Mass Ratio, (c) Velocity at Infinity, (d) Closest Approach to the Earth, (e) Initial Binary Semi-major Axis, (f) Initial Binary Orbit Eccentricity

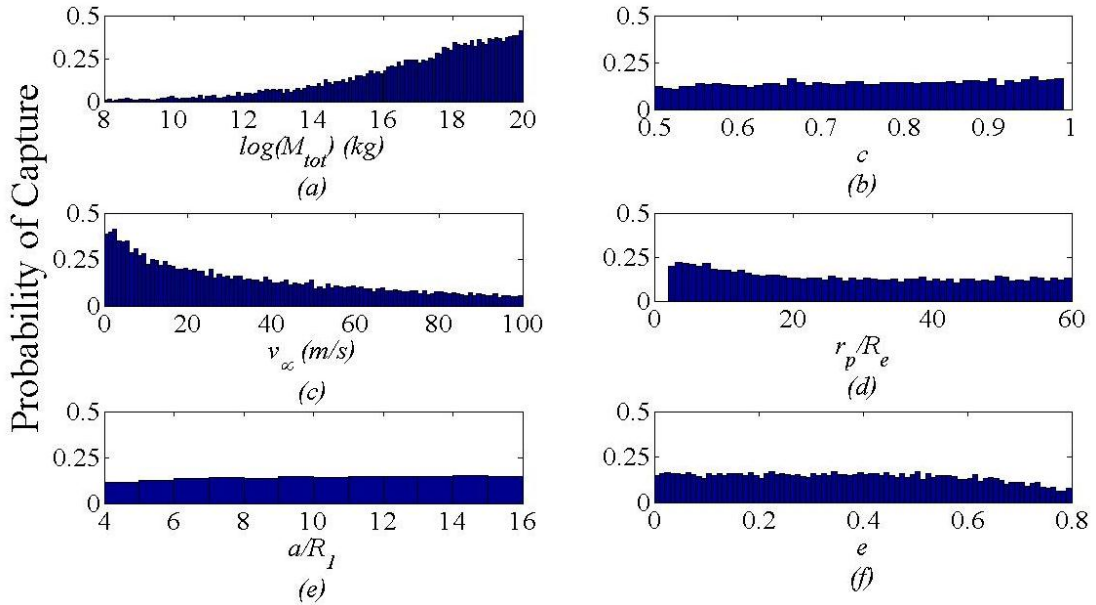


Figure 5. Probability of Capture as a Function of the System Variables for Smaller Binary Member. (a) Total Mass, (b) Mass Ratio, (c) Velocity at Infinity, (d) Closest Approach to the Earth, (e) Initial Binary Semi-major Axis, (f) Initial Binary Orbit Eccentricity

These trends should be expected, as binary systems with lower v_∞ have less total energy, and therefore less energy loss is required for capture to occur. Binaries with higher total masses rotate at faster rates than those with lower masses. Thus, at the closest approach, the asteroid closest to the Earth will be moving slower relative to the Earth (see Figure 1). Smaller close

approaches result in higher probability of capture since the tidal forces responsible for disrupting the binary and pulling one member into a permanent orbit are stronger. The trends observed in a and e can be attributed to greater probability of collision at low a and high e , as the two asteroids had closer encounters in these regions.

The next group of plots displays the resulting semi-major axes of the captured asteroids as functions of the system variables. Figure 6 represents data for the larger binary members, while Figure 7 represents data for the smaller member. The horizontal red line in each plot corresponds to half the radius of the Earth's Hill sphere. In order for the asteroid's orbit to be contained within the Earth's Hill sphere, its semi-major axis must be below this red line.

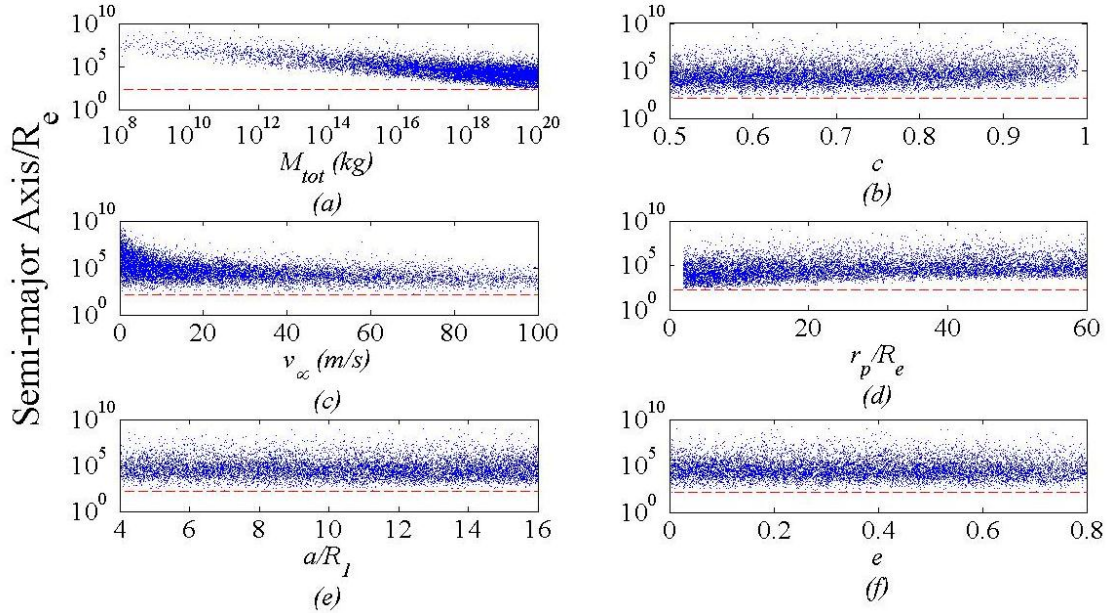


Figure 6. Resulting Semi-major Axis of Captured Asteroids as a Function of the System Variables for Larger Binary Member. (a) Total Mass, (b) Mass Ratio, (c) Velocity at Infinity, (d) Closest Approach to the Earth, (e) Initial Binary Semi-major Axis, (f) Initial Binary Orbit Eccentricity

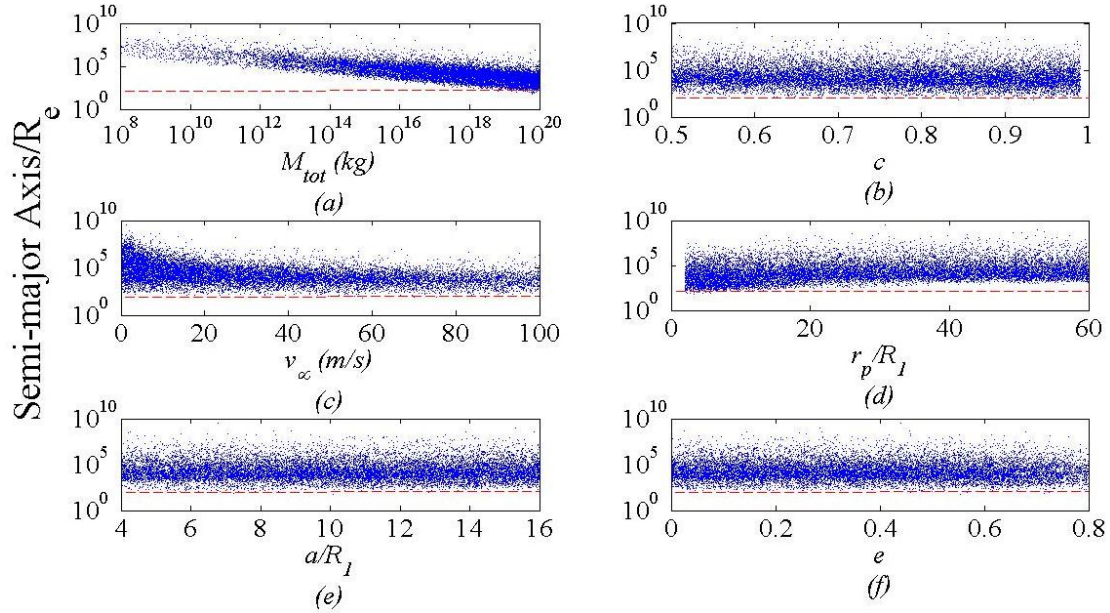


Figure 7. Resulting Semi-major Axis of Captured Asteroids as a Function of the System Variables for Smaller Binary Member. (a) Total Mass, (b) Mass Ratio, (c) Velocity at Infinity, (d) Closest Approach to the Earth, (e) Initial Binary Semi-major Axis, (f) Initial Binary Orbit Eccentricity

The resulting semi-major axes of the smaller member tend to be smaller than those of the larger member, and the plots are denser for the smaller member, again showing a higher probability of capture. Some trends can be seen in each variable; however, the total mass is the dominant variable in determining the size of the orbits. Figure 8 contains plots showing v_∞ vs. M_{tot} for the smaller and larger binary members. These are the most important variables affecting the probability of capture and the size of the resulting orbit. In the plots, a blue mark represents a captured asteroid, a red mark represents an uncaptured asteroid, and a green mark represents a collision between the two asteroids.

There are distinct regions for both members in which capture is more likely to occur. For a given binary system of know total mass, the plots below can be used to determine the maximum v_∞ at which capture can occur. Simulations conducted in two dimensions exhibited the same trends as those observed in three dimensions.

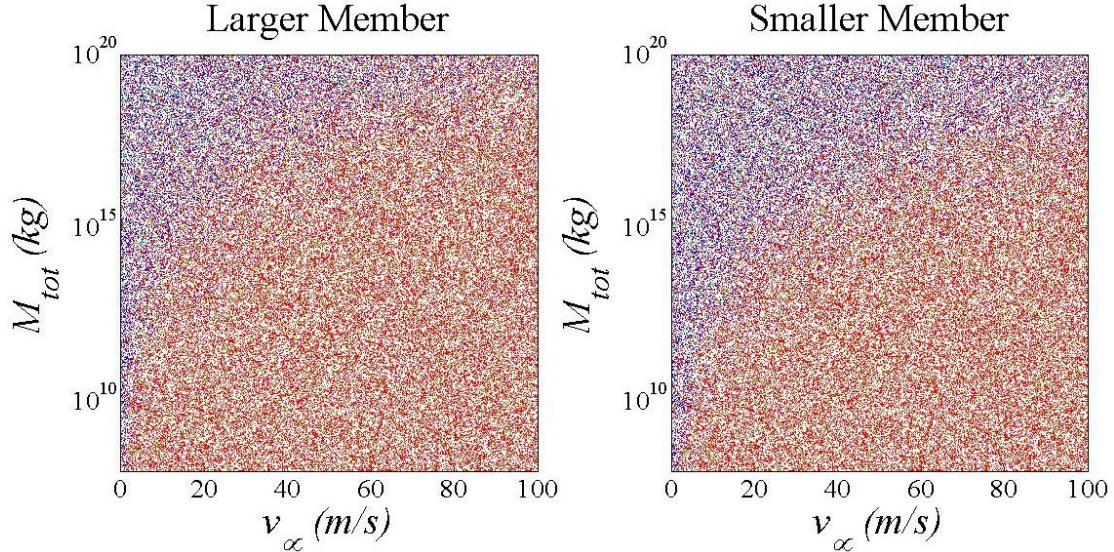


Figure 8. Capture Distribution over M_{tot} vs. v_{∞}

6. Choice of Candidate Asteroid

From the results presented in the previous section, it is clear that the total mass of the binary system has the largest impact on the probability of capture and the size of the resulting orbits. For this reason, we propose that the best candidate near-Earth binary asteroid for capture is 1999 HF1. This is the most massive of the known near-Earth binary asteroids, with a total mass of 6.7×10^{13} kg. The mass ratio of this binary is 0.988, and the orbital semi-major axis is 6 km^{22} . In the following sections, results of simulations considering this particular binary asteroid are presented. In these simulations, the eccentricity of the binary system was assumed to be 0. Therefore, θ was not varied, as varying θ and α are the same for circular orbits.

In the previous section, each simulation involved eleven initial conditions and binary parameters. When considering just one binary asteroid, the total mass, mass ratio, initial semi-major axis, and initial eccentricity are known, thus reducing the number of unknowns in each simulation to seven. The results from the previous section suggest that the binary asteroid 1999 HF1 is too small for binary exchange to be successful. However, we can now test over a finer grid of initial conditions since only seven unknowns are involved in each simulation, with the hope that this higher resolution in the parameter space will produce capture at a total mass of 6.7×10^{13} kg.

7. Candidate Asteroid Simulations

In Section 5, many different total binary masses, mass ratios, and initial semi-major axes were considered. Therefore, no critical value of close approach was observed in the data. However, now that only one binary system is being considered, we expected to observe some

tidal radius, below which capture is more likely to occur. In previous literature^{13,14,15}, an approximation of this tidal radius has been given by,

$$r_{td} = a \left(\frac{3M_p}{m_1 + m_2} \right)^{1/3} \quad (2)$$

where m_1 and m_2 are the masses of the two members of the binary and M_p is the mass of the planet. For the binary asteroid 1999HF1, this tidal radius is 6.02 Earth radii. Figures 9 and 10 show the probability of capture as functions of v_∞ and r_p for the larger and smaller members of the binary, respectively. On the plot of probability of capture vs. r_p , the tidal radius is marked by a vertical red line.

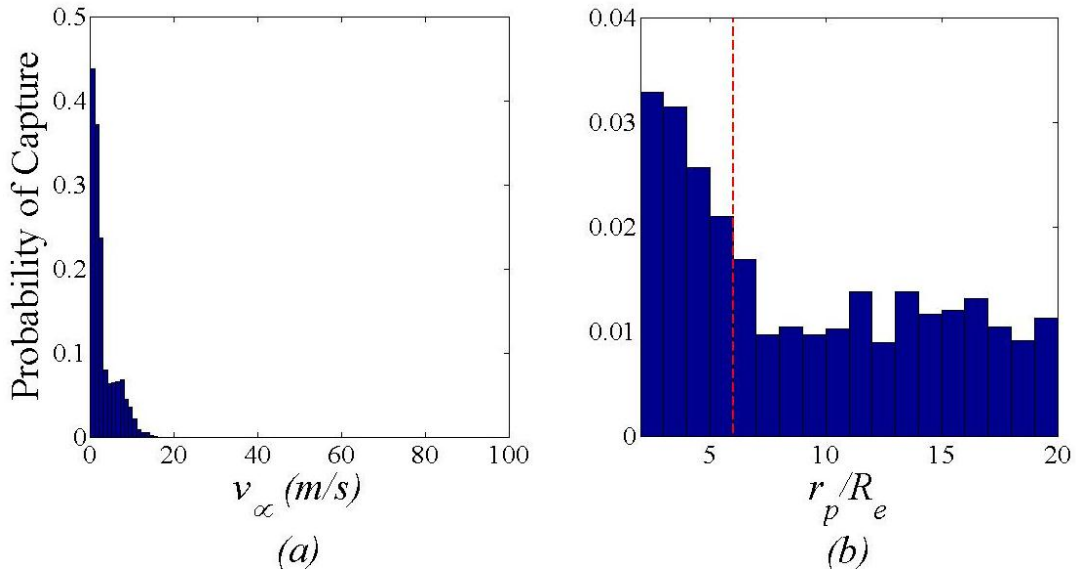


Figure 9. Probability of Capture as a Function of the System Variables for Larger Binary Member. (a) Velocity at Infinity, (b) Closest Approach to the Earth

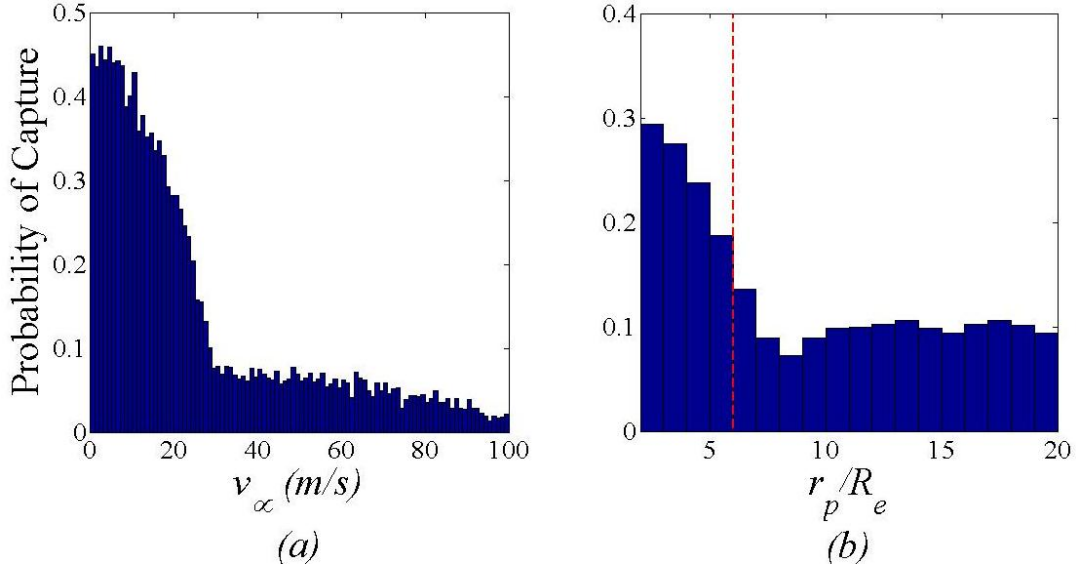


Figure 10. Probability of Capture as a Function of the System Variables for Smaller Binary Member. (a) Velocity at Infinity, (b) Closest Approach to the Earth

For the larger mass, the probability of capture drops quickly as v_∞ is increased and is slightly higher for smaller close approaches (note that the range in plot (b) for the larger mass is only 0% to 4%, while it is 0% to 40% for the smaller mass). For the smaller mass, the probability of capture drops below 10% above $v_\infty = 30$ m/s, and is highest when r_p is less than 6 Earth radii, which agrees with the theoretical prediction.

Figures 11 and 12 present the resulting semi-major axes from simulations that resulted in capture as functions of v_∞ and r_p for the larger and smaller members of the binary, respectively. As in Figures 6 and 7, half the radius of the Hill sphere is marked by the horizontal red line. On the plot of semi-major axis vs. r_p , the tidal radius is marked by a vertical green line.

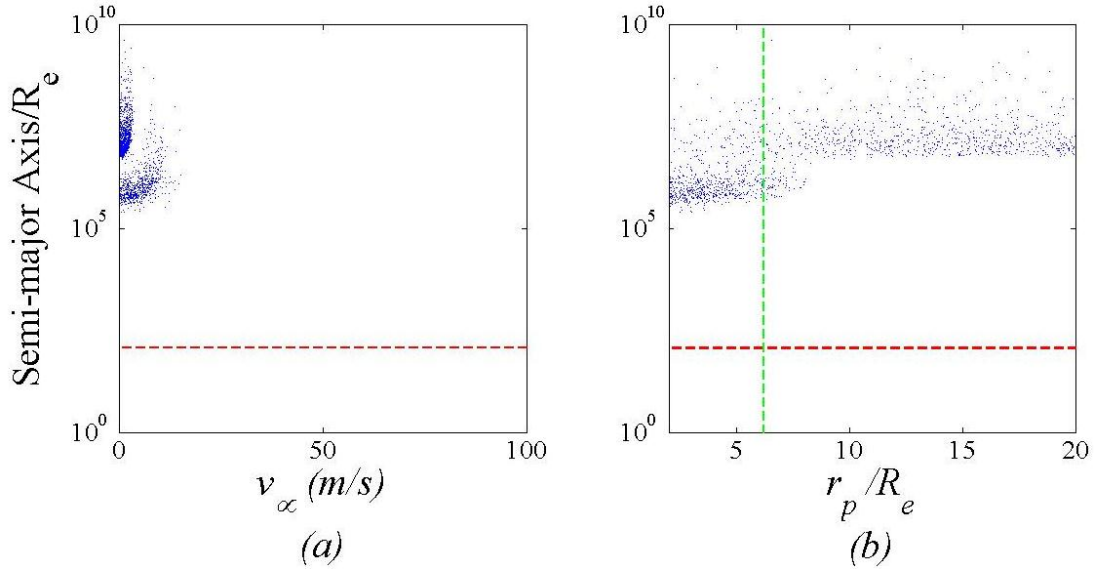


Figure 11. Resulting Semi-major Axis of Captured Asteroids as a Function of the System Variables for Larger Binary Member. (a) Velocity at Infinity, (b) Closest Approach to the Earth

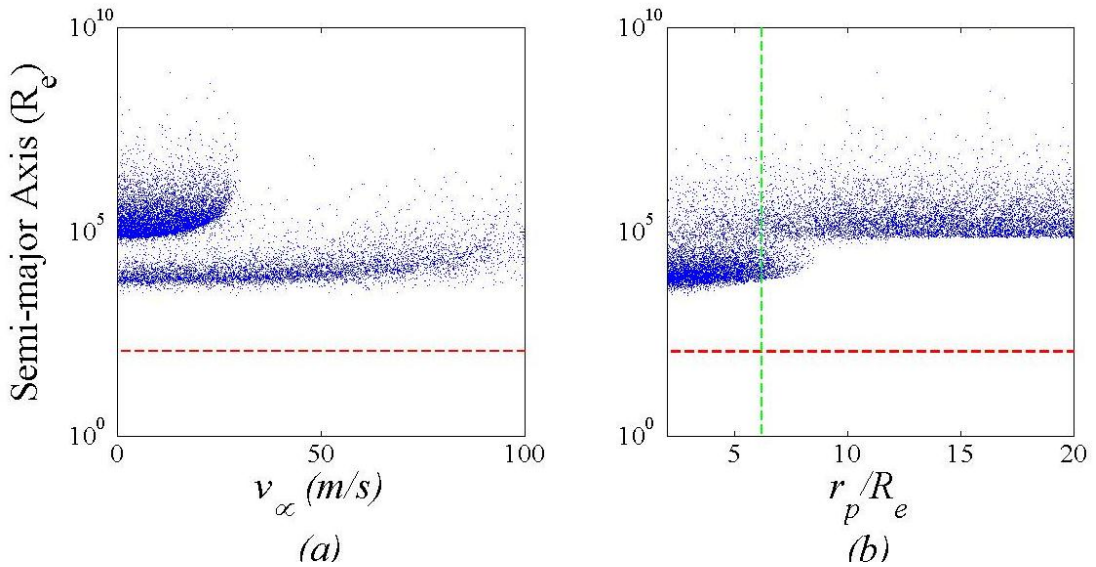


Figure 12. Resulting Semi-major Axis of Captured Asteroids as a Function of the System Variables for Smaller Binary Member. (a) Velocity at Infinity, (b) Closest Approach to the Earth

These plots show that the smallest resulting semi-major axes occur when the close approach is less than the tidal radius. We also observe two bands on the v_∞ plot for each asteroid. The lower bands in the v_∞ plots correspond to close approaches less than the tidal radius. The higher bands in the v_∞ plots correspond to close approaches greater than the tidal radius. Again, these findings agree with the theoretical prediction given by Equation 2. Figure 13 displays

captured and uncaptured data points for r_p and v_∞ . The colors have the same meaning as in Figure 8. The tidal radius is marked by a horizontal black line.

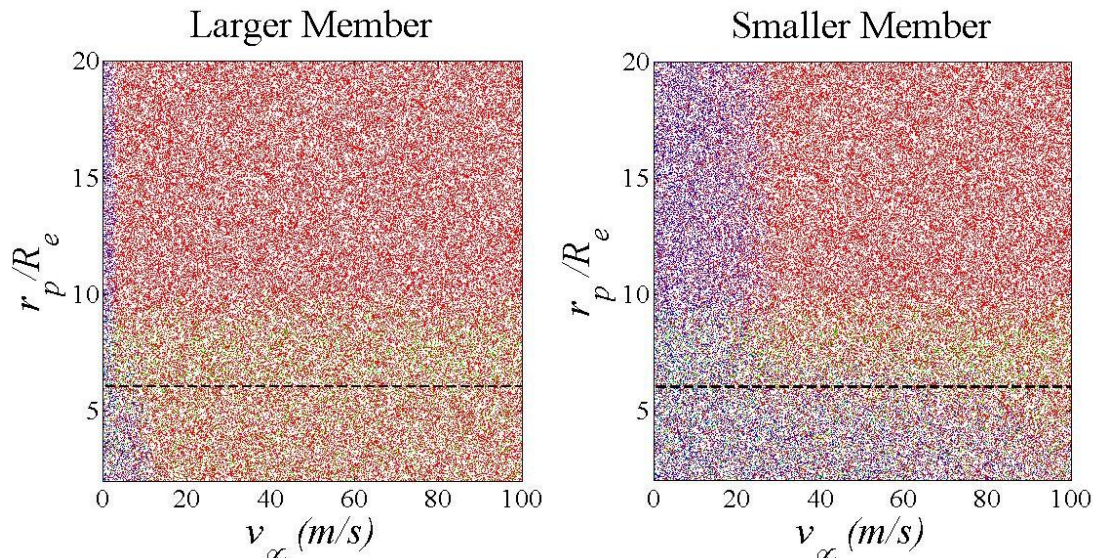


Figure 13. Capture Distribution over r_p vs. v_∞

If the binary asteroid's approach to the Earth is less than the tidal radius, the range of v_∞ in which capture can occur is greatly increased. Also, the probability of collision is much greater just above the tidal radius, as can be seen by the concentration of green data points. Again, two dimensional simulations exhibited the same trends.

While these results show that capture is possible with the candidate binary asteroid, the orbits of the captured asteroids all extend well outside of the Earth's Hill sphere. Looking back at the data presented in Section 5, we see that capture is possible within the Hill sphere with asteroids larger than the chosen candidate asteroid. However, these larger non-near-Earth binary asteroids would be much more difficult to reach, and steering them onto an orbit with a close approach to the Earth would be much more difficult compared to a near-Earth binary asteroid.

8. Extended Body Effects

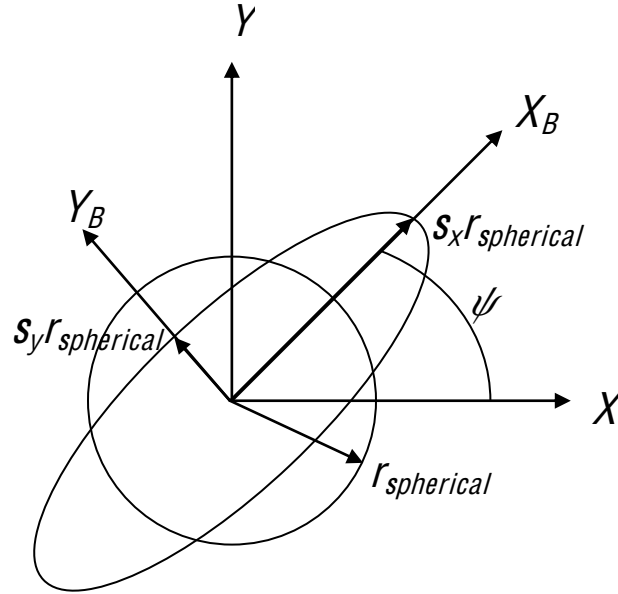
While some binary asteroid members can be nearly spherical, it is also possible for them to have elongated shapes. To convey a more accurate dynamic relation between non-spherical binary members, a higher order gravitational potential field was implemented into the model. Prior to implementing this gravitational field model, only point mass gravitational field models had been used to represent the gravitational interaction of the binary. The extended body approach offers a detailed description of the gravitational interaction between the two bodies of the binary by taking into account the rotation and physical shape of the larger asteroid. MacCullagh's gravity potential approximation²⁵(shown in Equation (3)) was chosen because it added the desired degree of precision, without incorporating unnecessary complexity into the model. In addition, an axially symmetric geometry was chosen so that the physical shape of the

body could be varied and to simplify the mathematical description of the potential without compromising the insight gained from the higher order approximation.

$$V(r) = -\frac{Gm}{r} - \frac{G}{2r^3} \left[I_{xx} \left(1 - 3 \frac{x^2}{r^2} \right) + I_{yy} \left(1 - 3 \frac{y^2}{r^2} \right) \right] \quad (3)$$

Here, I_{xx} and I_{yy} are the principal moments of inertia and x and y are the distances between the two asteroids in the body fixed principal axis frame of the larger member.

25,000 simulations using this new gravity potential were conducted in two dimensions (so $\beta = \gamma = 0$) using the candidate asteroid. To vary the shape of the larger asteroid, the radius of the asteroid was calculated as if it were spherical. Then this radius was multiplied by stretching factors s_x and s_y in the x and y directions of the body fixed frame to create an ellipsoidal shape, as shown in Figure 14.



An angle, ψ , giving the initial orientation of the larger member was also chosen. The new variables were chosen using the Latin hypercube method in the ranges $s_x \in [-0.9, 0.9]$, $s_y \in [-0.9, 0.9]$, and $\psi \in [0, 2\pi]$. Figures 15-18 show the probability of capture and resulting semi-major axes as functions of v_∞ and r_p for the larger and smaller binary members. The overall trends seen in these plots agree with those seen in the previous section. Thus, treating the larger binary member as an extended body has little effect on capture.

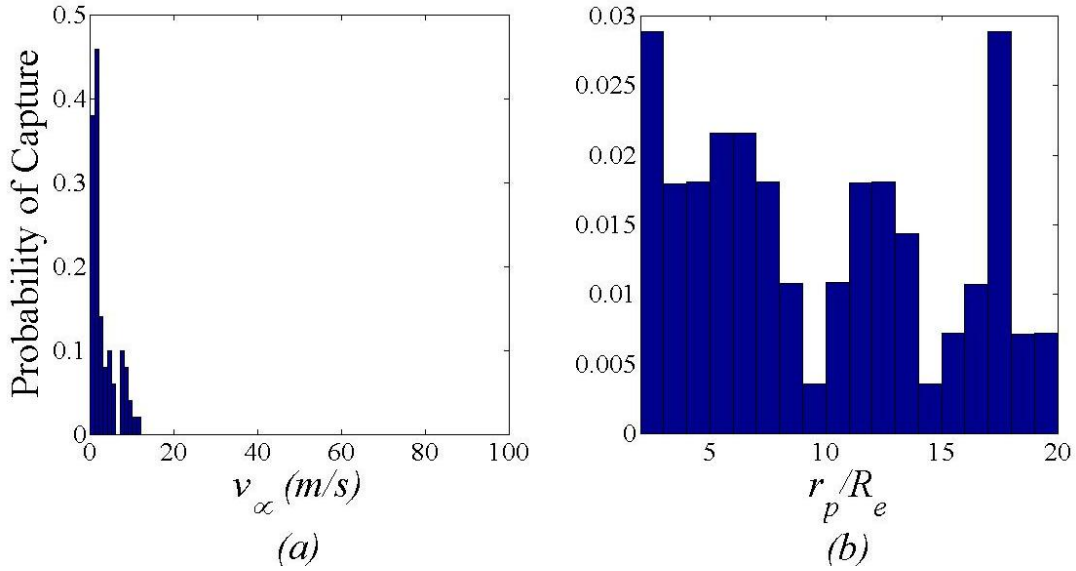


Figure 15. Probability of Capture as a Function of the System Variables for Larger Binary Member. (a) Velocity at Infinity, (b) Closest Approach to the Earth

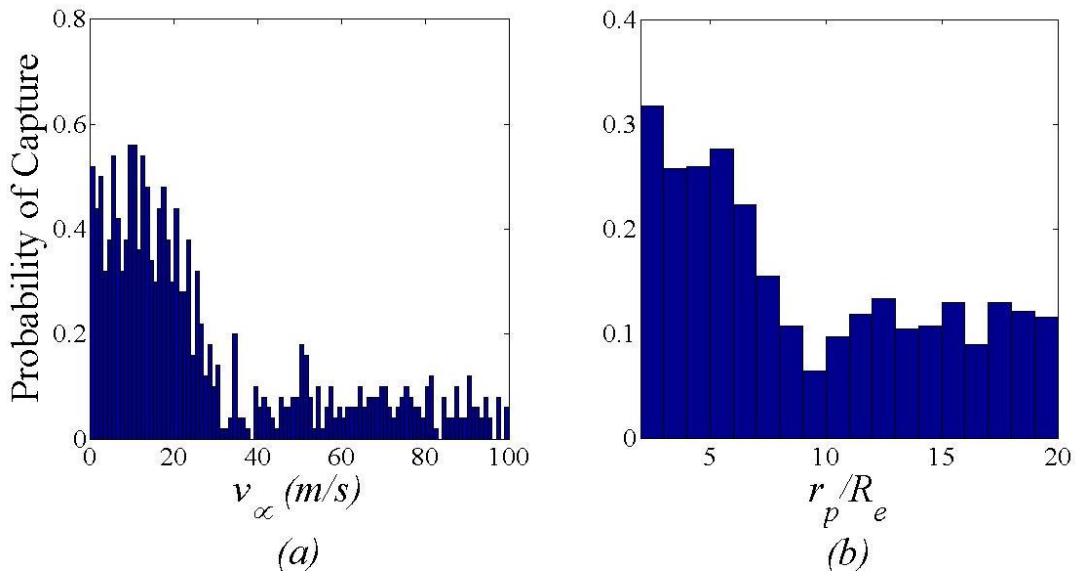


Figure 16. Probability of Capture as a Function of the System Variables for Smaller Binary Member. (a) Velocity at Infinity, (b) Closest Approach to the Earth

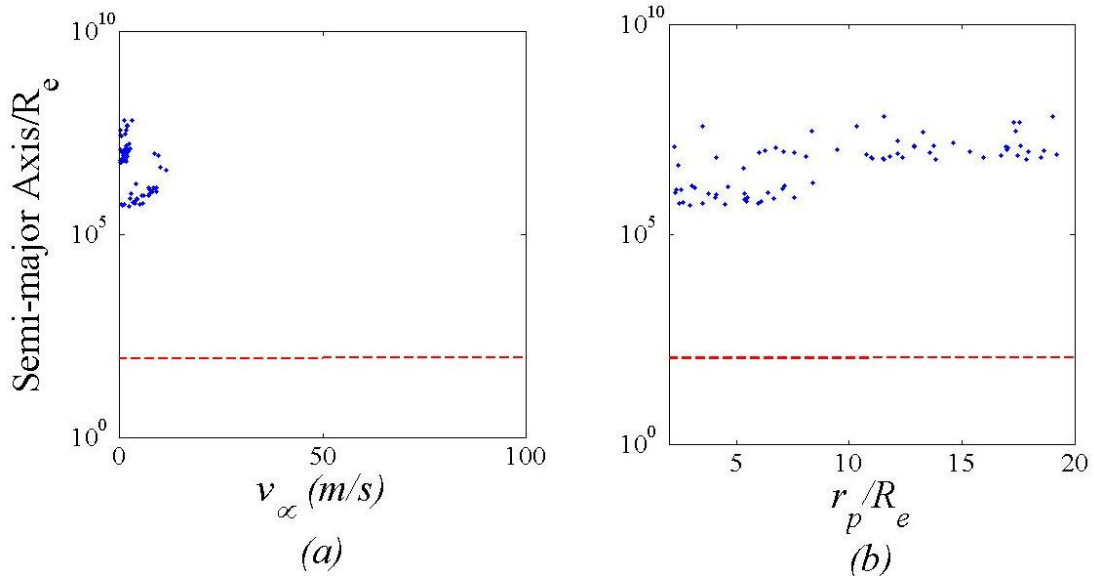


Figure 17. Resulting Semi-major Axis of Captured Asteroids as a Function of the System Variables for Larger Binary Member. (a) Velocity at Infinity, (b) Closest Approach to the Earth

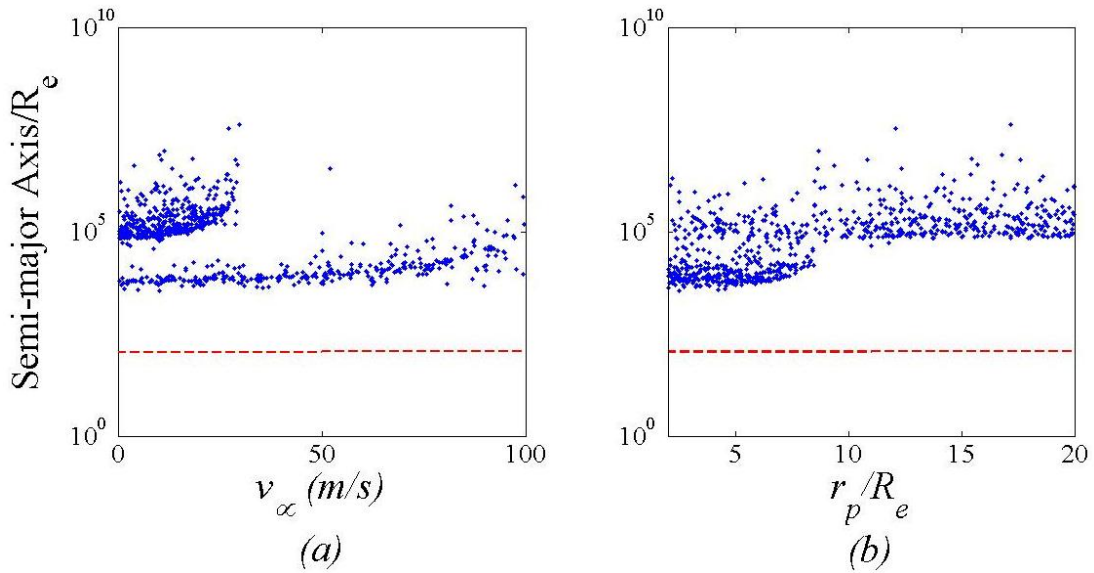


Figure 18. Resulting Semi-major Axis of Captured Asteroids as a Function of the System Variables for Smaller Binary Member. (a) Velocity at Infinity, (b) Closest Approach to the Earth

9. Effects of the Moon

50,000 two dimensional simulations were also conducted with the effect of the moon included. When the binary asteroid did not have a close approach with the moon, the moon caused a small change in the phase of the binary asteroid as it passed by the Earth. Capture is very sensitive to this phase. However, the overall statistical data presented earlier was unchanged when the binary asteroid did not have a close approach with the moon.

When the asteroid did have a close approach with the moon, i.e. entered the moon's Hill sphere, which as a radius of approximately 6×10^4 km, the moon had an outstanding effect on the binary asteroid pair. The asteroids that had close approaches to the moon were sometimes disrupted and one member was captured on an orbit contained within the Earth's Hill sphere. In some instances, the binary was not disrupted, and both members were captured on permanent orbits within the Earth's Hill sphere. Other simulations in which the binary asteroid had a close approach with the moon did not result in capture. This phenomenon resulted in much higher probabilities of capture over the ranges of v_∞ and r_p . The captured, but undisturbed binary asteroid result suggests that this mechanism could also work for a single asteroid.

Figures 19 and 20 show the probability of capture as functions of v_∞ and r_p for the larger and smaller asteroids with the effects of the moon included.

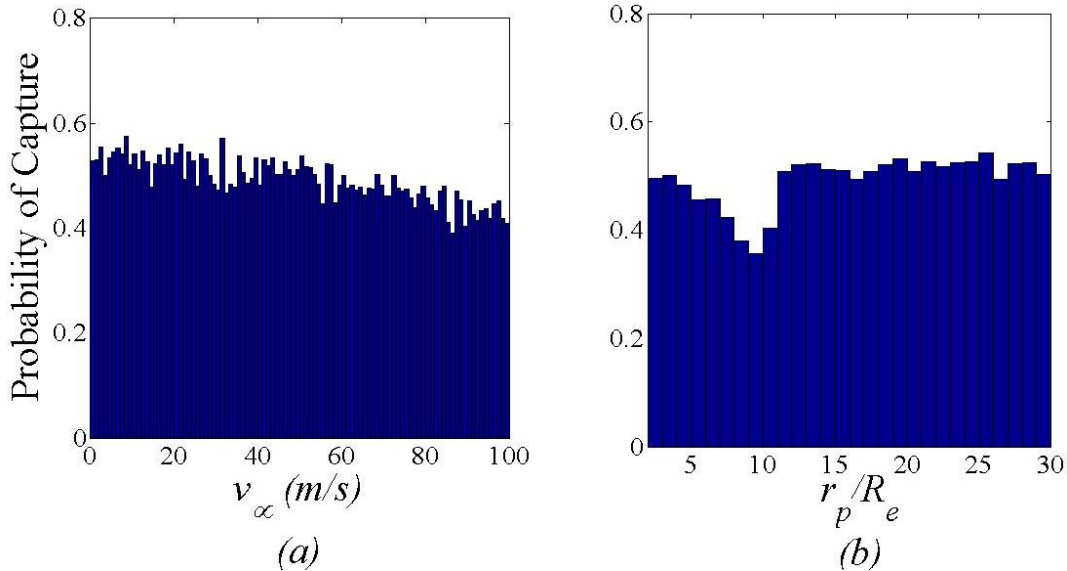


Figure 19. Probability of Capture as a Function of the System Variables for Larger Binary Member. (a) Velocity at Infinity, (b) Closest Approach to the Earth

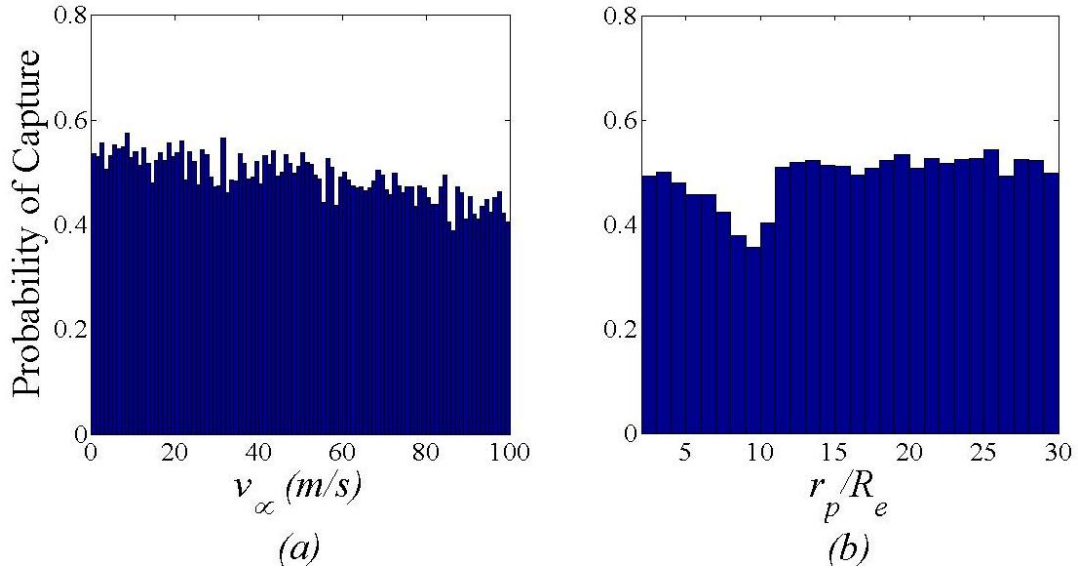


Figure 20. Probability of Capture as a Function of the System Variables for Smaller Binary Member. (a) Velocity at Infinity, (b) Closest Approach to the Earth

Figures 21 and 22 show the resulting semi-major axis of captured members as functions of v_∞ and r_p for the larger and smaller asteroids.

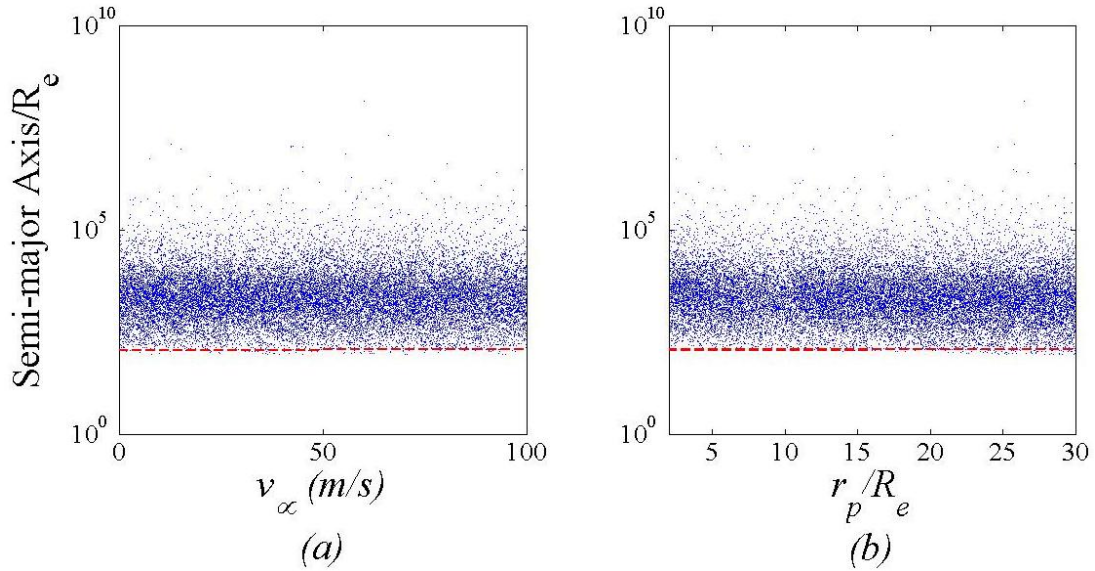


Figure 21. Resulting Semi-major Axis of Captured Asteroids as a Function of the System Variables for Larger Binary Member. (a) Velocity at Infinity, (b) Closest Approach to the Earth

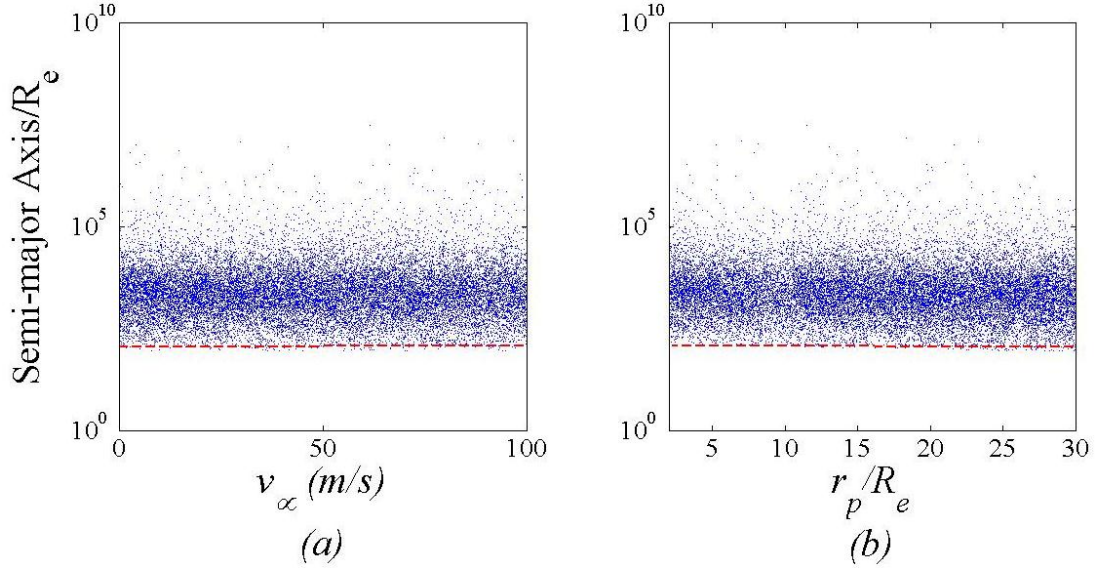


Figure 22. Resulting Semi-major Axis of Captured Asteroids as a Function of the System Variables for Smaller Binary Member. (a) Velocity at Infinity, (b) Closest Approach to the Earth

Figure 23 shows a single asteroid being captured with via a flyby of the moon. Since the captured asteroid is much less massive than the Earth and the moon, this system is a case of the restricted circular three body problem. The dynamics governing this three body system are much simpler than those governing the binary-Earth three body system, since the motion of the asteroid has a negligible effect on the moon and the Earth. A great deal of work has been done on the restricted circular three body problem which could be applied to this system²⁶, and analytical solutions for the initial conditions needed for capture may be obtainable. Further investigation must be undertaken to fully understand this moon assist phenomenon. The asteroid in Figure 23 has a velocity at infinity of $v_\infty = 1000$ m/s, which is much higher than the v_∞ considered for binary exchange earlier. This v_∞ is comparable to some actual v_∞ of near-Earth asteroids¹¹.

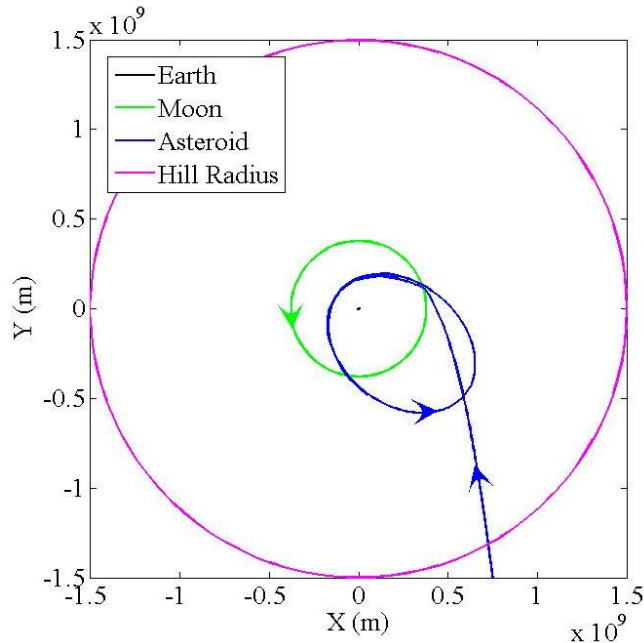


Figure 23. Asteroid Capture via a Moon Flyby (Movie available at <http://www.youtube.com/watch?v=6PWwtMnhd0A>)

10. Conclusions

A parametric study of binary-Earth encounters was conducted, and the results showed that the total binary mass and the approach velocity were the two dominant parameters affecting capture. This led to the choice of 1999 HF1 as a candidate near-Earth binary asteroid for capture, due to its large mass. Simulations with the candidate asteroid showed that while capture is possible, it only occurred at low v_{∞} , and the resulting orbits extend beyond the Earth's Hill sphere. Non-near-Earth binary asteroids with larger masses than the candidate asteroid could be captured within the Hill sphere. Treating the larger member of the candidate binary as an extended body had little effect on capture. Including the moon in the simulations allowed for capture within the Hill sphere when the binary asteroid had a close approach with the moon. Work on the restricted three-body problem suggests this moon-assisted Earth capture mechanism will work for single asteroids of nearly any size.

In addition to assessing the feasibility of intentional asteroid capture, this work also suggests that the natural capture of a moon through binary exchange, as has been suggested for Neptune and Jupiter, is very unlikely, since the near-Earth binary asteroids are too small for binary exchange to be successful. However, a close encounter between a single near-Earth asteroid and the moon could lead to the natural capture of another moon. Future work could be directed toward understanding this moon assist phenomenon and applying it to a single near-Earth asteroid. Work could also be done on the feasibility of steering a non-near-Earth binary asteroid onto an orbit with a close approach with the Earth

11. Acknowledgement

We would like to thank Dr. Shane Ross for his guidance and suggestions as he served as our project supervisor. We are also gracious for funding provided by the Virginia Space Grant Consortium and the Department of Engineering Science and Mechanics. We would finally like to extend thanks to Dr. Marie Parette, Dr. Jack Lesko, our Engineering Science and Mechanics classmates, and the Laboratory for Interdisciplinary Statistical Analysis (LISA) at Virginia Tech, particularly Nels Johnson and Kelly Geyer, for their useful input and advice.

References

1. Canup, R. and Ward, W., 2002, "Formation of the Galilean Satellites: Conditions of Accretion", *The Astronomical Journal*, 124, 3404-3423.
2. Jewitt, D. and Sheppard, S., 2004, "Irregular Satellites in the Context of Planet Formation", *Space Science Reviews*, 114, 407-421.
3. Brown, L., 2008, *Plan B 3.0*, W.W. Norton , New York, NY.
4. Creola, P., 1996, "Space and the fate of humanity", *Space Policy*, 12, 193-201.
5. Lewis, J., 1997, *Mining The Sky: Untold Riches From The Asteroid, Comets, And Planets*, Addison-Wesley Publishing Company, Boston, MA.
6. Kargel, J., 1994, "Metalliferous asteroids as potential sources of precious metals", *Journal of Geophysical Research*, 99, 129-141.
7. Busch, M., 2004, "Profitable Asteroid Mining", *Journal of the British Interplanetary Society*, 57, 301-305.
8. Sonter, M, 1997, "The Technical and Economic Feasibility of Mining Near-Earth Asteroids", *Acta Astronautica*, 41, 637-647.
9. Sanchez, J., McInnes, C., 2012, "Assessment of the Feasibility of Future Shepherding of Asteroid Resources", *Acta Astronautica*, 73, 49-66.
10. Massonnet, M. and Meyssignac, B., 2006, "A Captured Asteroid: Our David's Stone for Shielding Earth and Providing the Cheapest Extraterrestrial Material", *Acta Astronautica*, 59, 77-83.

11. Hasnain, Z., Lamb, C., and Ross, S., “Capturing Near-Earth Asteroid Around Earth”, preprint.
12. Friedman, G., 2005, “Comparing Mass Driver and Disperser concepts for non-nuclear mitigation of asteroid threat”, *Journal of the British Interplanetary Society*, 58, 310-315.
13. Gaspar, H., Winter, O., and Neto, E., 2011, “Irregular Satellites of Jupiter: Capture Configurations of Binary-Asteroids”, *Monthly Notices of the Royal Astronomical Society*, 415, 1999-2008.
14. Philpott, C., Hamilton, D., and Agnor, C., 2010, “Three-Body Capture of Irregular Satellites: Applications to Jupiter”, *Icarus*, 208, 824-836.
15. Agnor, C. and Hamilton, D., 2006, “Neptune’s Capture of its Moon Triton in a Binary-Planet Gravitational Encounter”, *Nature*, 441, 192-194.
16. Morbidelli, A., 2006, “Interplanetary Kidnap”, *Nature*, 441, 162-163.
17. Jewitt, D. and Haghighipour, N., 2007, “Irregular Satellites of the Planets: Products of Capture in the Early Solar System”, *Annual Review of Astronomy and Astrophysics*, 45, 261-295.
18. Nesvorny, D., Vokrouhlicky, D., and Morbidelli, A., 2007, “Capture of Irregular Satellites during Planetary Encounters”, *The Astronomical Journal*, 133, 1962-1976.
19. Neto, E. and Winter, O., 2009, “Gravitation Capture of Asteroids by Gas Drag”, *Mathematical Problems in Engineering*, 897570.
20. Neto, E., Winter, O., and Yokoyama, T., 2006, “Effect of Jupiter’s Mass Growth on Satellite Capture”, *Astronomy and Astrophysics*, 452, 1091-1097.
21. Cuk, M. and Gladman, B., 2006, “Irregular Satellite Capture during Planetary Resonance Passage”, *Icarus*, 183, 362-372.
22. Pravec, P. and Harris, A., 2007, “Binary Asteroid Population”, *Icarus*, 190, 250-259.
23. Press, W., Teukolsky, S., Vetterling, W., Flannery, B., 1992, *Numerical Recipes in Fortran 77: The Art of Scientific Computing*, pp. 718-725, Cambridge University Press, New York, NY.

24. McKay, M., Beckman, R., Conover, W., 1979, “A Comparison of Three Methods for Selecting Values of Input Variables in the Analysis of Output from a Computer Code”, *Technometrics*, 21, 239-245.
25. Schaub, H. and Junkins, J., 2009, *Analytical Mechanics of Space Systems, 2nd edition*, pp. 541-545, American Institute of Aeronautics and Astronautics, Reston, VA.
26. Koon, W.S., Lo, M.W., Marsden, J.E., Ross, S.D., 2008, *Dynamical Systems, the Three-Body Problem and Space Mission Design*.

Appendix 1. Near-Earth Binary Asteroid Data

Binary Asteroid	Orbital Semi-major Axis (km)	Mass of Body 1 (kg)	Mass of Body 2 (kg)	Total Mass (kg)	Mass Ratio M_1/M_{tot}
Apollo		7.71732E+12	662679700.4	7.71799E+12	0.999914138
Sisyphus					
Dionysus	4	5.30144E+12	42411500823	5.34385E+12	0.992063492
Sekhmet	1.5	1.5708E+12	42411500823	1.61321E+12	0.973709834
Ishtar	2.7	2.71434E+12	1.9635E+11	2.91069E+12	0.932541824
1998 PG	1.5	1.14511E+12	61738578828	1.20685E+12	0.948843166
1991 VH	3.6	2.71434E+12	1.43139E+11	2.85747E+12	0.949907236
Didymos	1.1	6.6268E+11	7717322354	6.70397E+11	0.98848843
1998 RO1	1.4	8.04248E+11	86192736044	8.9044E+11	0.903202134
1999 KW4	2.5	3.30966E+12	1.18889E+11	3.42855E+12	0.965323912
Hermes	1.2	3.39292E+11	2.47344E+11	5.86636E+11	0.578368999
1999 DJ4	0.7	67347892511	7717322354	75065214865	0.897191764
2001 SL9	1.5	8.04248E+11	16725839288	8.20974E+11	0.979626823
1994 CC		4.3138E+11	1570796327	4.32951E+11	0.996371882
1999 HF1	6	6.73479E+13	8.04248E+11	6.81521E+13	0.98819923
2001 SN263		3.0918E+13	1.5708E+12	3.24888E+13	0.951651114
1990 OS	0.7	42411500823	143138815.3	42554639639	0.996636352
2003 YT1	3.2	1.5708E+12	9160884178	1.57996E+12	0.994201815
1996 FG3	2.8	5.30144E+12	1.52895E+11	5.45433E+12	0.971968151
2000 DP107	2.9	8.04248E+11	56449707596	8.60697E+11	0.934413993
2002 CE26	4.7	6.45026E+13	42411500823	6.4545E+13	0.999342916
1994 AW1	2.4	1.5708E+12	1.73718E+11	1.74451E+12	0.900420677
1994 XD		3.39292E+11	5301437603	3.44593E+11	0.984615385
1998 ST27		8.04248E+11	2714336053	8.06962E+11	0.996636352
2000 CO101		2.20867E+11	143138815.3	2.2101E+11	0.999352341
2000 UG11	0.5	27608316240	5301437603	32909753843	0.838909837
2002 BM26		3.39292E+11	1570796327	3.40863E+11	0.995391705
2002 KK8		1.9635E+11	1570796327	1.9792E+11	0.992063492
2003 SS84		2714336053	339292006.6	3053628059	0.888888889
2004 DC		42411500823	339292006.6	42750792830	0.992063492
2005 AB	3.8	1.07741E+13	1.52895E+11	1.0927E+13	0.986007576
2005 NB7	0.9	1.9635E+11	12566370614	2.08916E+11	0.939849624
2006 GY2	0.6	1.00531E+11	804247719.3	1.01335E+11	0.992063492
2006 VV2		9.16088E+12	1.9635E+11	9.35723E+12	0.979016283
2007 DT103	0.5	42411500823	1570796327	43982297150	0.964285714
2008 BT18					

Appendix 2. The Gragg-Bulirsch-Stoer Numerical ODE Solver

The Gragg-Bulirsch-Stoer method of numerical integration is one of the best known ways to efficiently compute an accurate approximation of the solution of a system of ordinary differential equations¹. Although many modifications can be made to improve the method, the explanation below provides the general idea of the method.

Consider the first order autonomous ordinary differential equation $y' = f(y)$ with initial condition $y(a) = y_0$ that we would like to solve numerically on some domain $t \in [a, b]$. We begin by dividing the domain $[a, b]$ into N subintervals each of length H . Now consider the first subinterval $[a, a + H]$. We first divide this subinterval into $n_1 = 2$ subintervals each of length $h_1 = H/2$. Beginning at $y(a)$, we apply the modified midpoint rule to obtain a numerical approximation of $y(a + H)$. The modified midpoint rule is given by Equation 1.

$$\begin{aligned}
 y_0 &= y(a) \\
 y_1 &= y_0 + hf(y_0) \\
 y_{i+1} &= y_{i-1} + 2hf(y_i) \quad i=1,2,\dots,n-1 \\
 y(a+H) &= \frac{1}{2}[y_n + y_{n-1} + hf(y_n)]
 \end{aligned} \tag{1}$$

Figure 1 shows an example of the modified midpoint method applied using 2 subintervals.

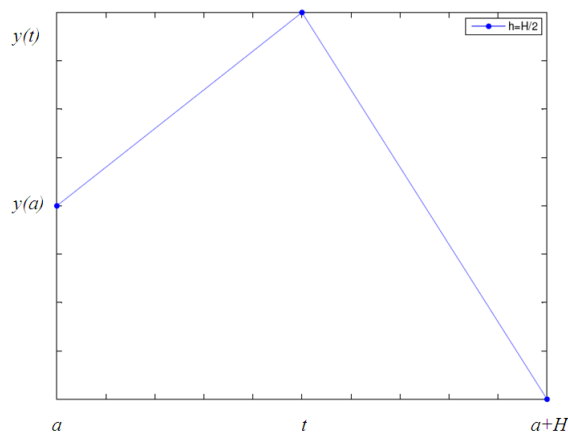


Figure 1

We now make a plot of $y(a + H)$ vs. h . The idea is to fit curves to our solutions on this plot and extrapolate them back to $h = 0$, which corresponds to taking infinitely many infinitesimal time steps. Figure 4 shows the $y(a + H)$ vs. h plot with the point obtained using $h = H/2$. Fitting a curve to this point provides a straight line passing the point.

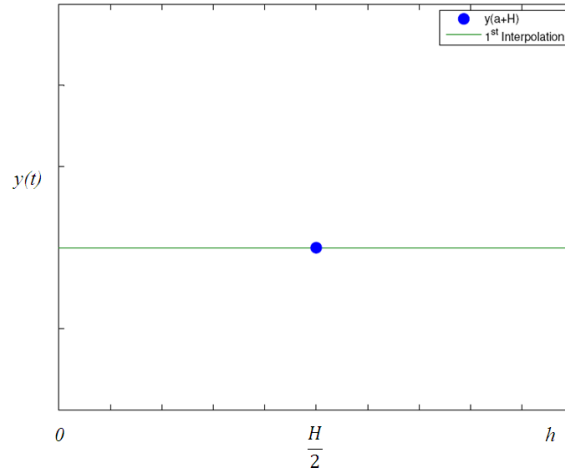


Figure 2

Next, we apply the modified midpoint rule on the interval $[a, a+H]$ again; however, the interval is now divided into $n_2 = 4$ subintervals each of length $h_2 = H/4$. We now have a better approximation of $\mathcal{J}(a+H)$, which is shown in Figure 3.

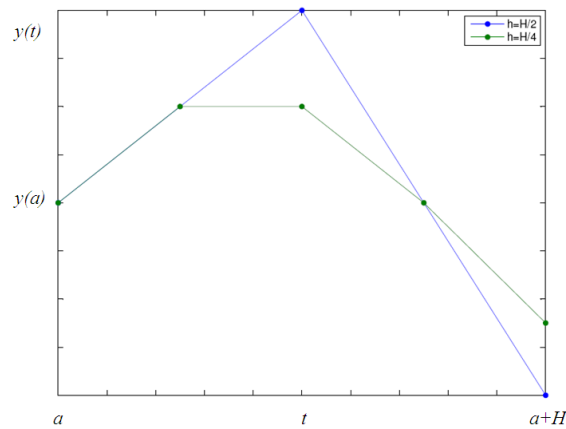


Figure 3

Figure 4 shows this point added to the $\mathcal{J}(a+H)$ vs. h plot and a linear interpolation of the two points.

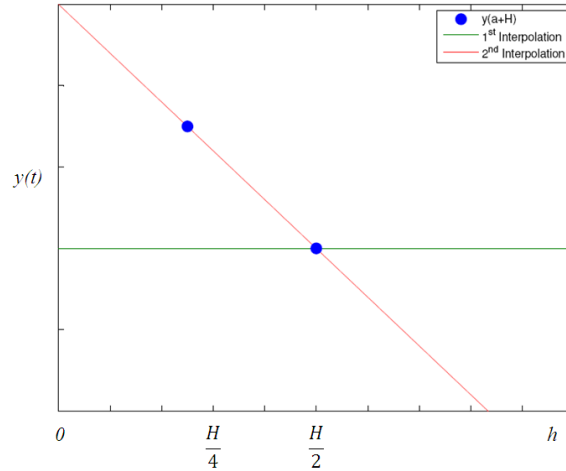


Figure 4

Our goal is to extrapolate these fitted functions back to $h=0$ to obtain a very accurate approximation of $y(a+H)$. As can be seen in Figure 4, there is a large discrepancy between the value obtained at $h=0$ for the function interpolating $h_1 = H/2$ and the function interpolating both $h_1 = H/2$ and $h_2 = H/4$. Thus we perform another iteration, this time with $n_3 = 8$, so that $h_3 = H/8$. We continue to do this until the current interpolating function and the previous interpolating function agree at $h=0$ to within some tolerance. Figure 5 shows the method continued up to $n_4 = 16$, so that $h_4 = H/16$.

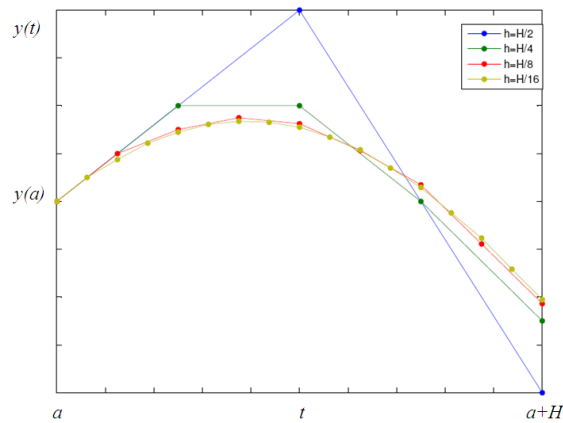


Figure 5

Figure 6 shows the interpolating functions for each set of data.

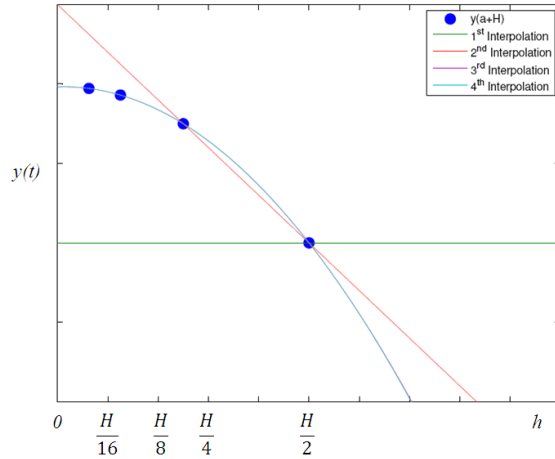


Figure 6

A horizontal line interpolates the point corresponding to h_1 , a linear line for h_1 and h_2 , a quadratic polynomial for h_1 , h_2 , and h_3 , and a cubic polynomial for h_1 , h_2 , h_3 , and h_4 . The cubic polynomial and the quadratic polynomial seem to agree well at $h=0$. Figure 7 shows a magnified view of the cubic and quadratic polynomials near $h=0$.

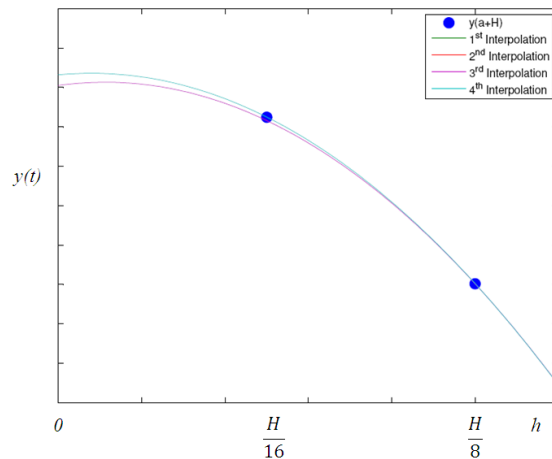


Figure 7

If the difference at $h=0$ is less than some specified tolerance, then this value is accepted to be $y(a+H)$. If the difference is greater than the tolerance, then another iteration is performed with $n_5 = 32$ and $h_5 = H/32$, and so on. Once the difference is below the tolerance and a solution has been reached, this solution is used as y_0 on the next interval of step size H . This process is continued until the solution at $y(a+NH) = y(b)$ is reached.

The advantage of this method over other algorithms is that large step sizes H can be used and an accurate approximation can still be obtained. These large step sizes greatly decrease the computing time needed to compute the solution of the ordinary differential equation. Also, this method provides a much more accurate solution than other methods, such as the fourth order Runge-Kutta Method. If k is the number of times the modified midpoint method is applied over

each interval of length H (i.e. n_k), then the method has a global error of order H^{2k-1} . Just a few iterations over each interval of length H can produce a solution of very high order.

One improvement that can be made is to adjust the large step size H after each time step. Formula (2) can be used to automatically adjust the step size based upon the tolerance and the error obtained during the previous iteration.

$$H_{i+1} = H_i \left(\frac{tol}{err} \right)^{\frac{1}{2k-1}} \quad (2)$$

Using this formula increases the time step in areas of the solution where convergence is reached quickly and decreases the time step in areas of the solution where convergence occurs slowly. This modification greatly increases the accuracy, stability, and efficiency of the integrator.

References

1. Press, W., Teukolsky, S., Vetterling, W., Flannery, B., 1992, *Numerical Recipes in Fortran 77: The Art of Scientific Computing*, pp. 718-725, Cambridge University Press, New York, NY.